J Neurophysiol 89: 177–185, 2003;
10.1152/jn.00667.2002.

Actions of U-92032, a T-Type Ca^{2+} Channel Antagonist, Support a Functional Linkage Between I_T and Slow Intrathalamic Rhythms

DARRELL M. PORCELLO, STEPHEN D. SMITH, AND JOHN R. HUGUENARD
Department of Neurology and Neurological Sciences, Stanford University Medical Center, Stanford, California 94305

Submitted 13 August 2002; accepted in final form 3 September 2002.

Porcello, Darrell M., Stephen D. Smith, and John R. Huguenard. Actions of U-92032, a T-type Ca^{2+} channel antagonist, support a functional linkage between I_T and slow intrathalamic rhythms. *J Neurophysiol* 89: 177–185, 2003; 10.1152/jn.00667.2002. Thalamic relay neurons express high levels of T-type Ca^{2+} channels, which support the generation of robust burst discharges. This intrinsically mediated form of phasic spike firing is thought to be critical in the generation of slow (3–4 Hz) synchronous oscillatory activity of absence epilepsy. Recordings made from brain slices or whole animals have shown that slow synchronous absence-like activity can be abolished when Ca^{2+}-dependent burst firing in relay neurons is interrupted by the pharmacological or genetic inactivation of T-channels. Because succinimide drugs act as incomplete and nonspecific antagonists, we tested whether the novel T-channel antagonist U-92032 could provide stronger support for a role of T-channels in slow oscillatory activity. Ca^{2+}-dependent rebound (LTS) bursts were recorded using whole cell current clamp in relay cells of the ventral basal complex (VB) from thalamic slices of adult rats. We used LTS kinetics to measure the availability of T-channels in VB cells after TTX. U-92032 (1 and 10 μM) reduced the maximum rate of depolarization of the isolated LTS by 51% and 90%, respectively, compared with the 35% reduction due to 2 mM methylphenylsuccinimide (MPS), the active metabolite of the antiabsence drug methsuximide. U-92032 (1 and 10 μM) also suppressed evoked, slow oscillations in thalamic slices with a time course similar for observed intracellular effects. Unlike MPS, we observed no substantial effects of short-term U-92032 applications ($\leq$2 h) on the generation of action potentials in VB cells. Our findings show U-92032 is a more potent, effective, and specific T-channel antagonist than previously studied succinimide antiabsence drugs and that it dramatically reduces epileptiform synchronous activity. This suggests that U-92032 or other specific T-channel antagonists may provide effective drug treatments for absence epilepsy.

INTRODUCTION

Cortical rhythmogenesis has a profound effect on routine brain functions such as attention, sensory transmission, and sleep. Multiple experimental approaches including brain lesions (Avanzini et al. 1993; Morison and Basset 1945; Vergnes et al. 1990), pharmacological perfusions (Avanzini et al. 1989, 1993), in vivo recordings (Gloor and Fariello 1988; Spiegel and Wycis 1950; Steriade et al. 1985; Vergnes et al. 1987; Williams 1953), and computational modeling (Destexhe and Sejnowski 1997) have suggested a central role for the thalamus in the transition of desynchronized cortical activity to a synchronized state. During sleep spindles, and slower, 3- to 4-Hz oscillations associated with absence epilepsy, the thalamocortical circuit is likely entrained by intrathalamic oscillations that are dependent on interactions between the thalamic reticular nucleus (RTN) and thalamocortical relay (TC) nuclei (Jahnsen and Llinas 1984; McCormick and Bal 1997; Steriade et al. 1993). While it has been shown for both intact thalamocortical systems and isolated cortex that synchronization can be driven by intracortical activity (Destexhe et al. 1999; Steriade and Contreras 1998), clear cellular mechanisms have been defined within thalamic circuits (see next paragraph) that likely support the genesis of thalamocortical absence seizures.

RTN and TC cells are reciprocally connected, with RTN cells providing inhibitory input onto excitatory TC cells (Jones 1985). Because TC cells can generate rebound bursts in response to inhibition, their excitatory output can complete a cycle of activity within the intrathalamic circuit (Steriade and Deschenes 1984; Ulrich and Huguenard 1997). A low threshold Ca^{2+}-conductance mediated by "transient" or T-type calcium channels (I_T) drives burst firing in both RTN and TC cells. Bursting produces robust synaptic outputs that sustain rhythmicity between the two thalamic cell groups and reinforce thalamocortical oscillatory activity (Huguenard and Prince 1994b; Jahnsen and Llinas 1984; von Krosigk et al. 1993).

A solid link between I_T and absence epilepsy has been established from experiments showing a deficit of $GABA_B$ agonist-dependent absence seizures in T-channel knockout mice (Kim et al. 2001), the upregulation of thalamic T-channels in rodent absence models (Talley et al. 2000; Tsakiridou et al. 1995; Song et al. 2001; Zhang and Noebels 2001;), and the rescue of one absence phenotype by crossing against a strain lacking the major form of thalamic T-channel (Song et al. 2001). Further support for this link comes from the reduction of I_T in acutely dissociated TC cells of the ventral basal complex (VB) by antiepileptic drugs (or their active metabolites), effective against absence epilepsy, including ethosuximide (ES), methsuximide, and trimethadione (Coulter et al. 1989, 1990).

As predicted by the hypothesis that T-channel–dependent bursting in thalamus is central to absence epilepsy when ES

Address for reprint requests: J. R. Huguenard, Dept. of Neurology and Neurological Sciences, Stanford University Medical Center, Stanford, CA 94305-5122 (E-mail: John.Huguenard@Stanford.EDU).

The costs of publication of this article were defrayed in part by the payment of page charges. The article must therefore be hereby marked "*advertisement*" in accordance with 18 U.S.C. Section 1734 solely to indicate this fact.

was applied to thalamic slices, the inhibition of I_T correlated with a network-level suppression of evoked experimental absence seizures (Huguenard and Prince 1994b; Kao and Coulter 1997). However, Leresche et al. (1998) have recently shown that other cellular actions, reductions in persistent Na^+ currents and/or Ca^{2+}-dependent K^+ currents, may play important roles in the anti-oscillatory effects of ES in thalamus. These and other findings have led to some controversy regarding the T-channel–dependent hypothesis of intrathalamic rhythmicity (reviewed in Crunelli and Leresche 2002; Huguenard 2002).

U-92032, (7-[[4-[bis(4-fluorophenyl)methyl]-1-piperazinyl]-methyl]-2-[(2-hydroxyethyl)amino]4-(1-methylethyl)-2,4,6-cycloheptatrien-1-one), has been shown to block I_T in guinea pig atrial cells (Xu and Lee 1994), mouse neuroblastoma cells (Ito et al. 1994), and isolated hippocampal CA1 pyramidal neurons (Avery and Johnston 1997). While the Ca^{2+}-current antagonism ascribed to U-92032 is specific for I_T compared with higher threshold currents at low concentrations (<10 μM), there is evidence for a significant effect on voltage dependent Na^+ channels, with 33% blockade at 1 μM (Avery and Johnston 1997). To provide additional pharmacological support of a central role for T-channels in intrathalamic rhythmicity, we show that U-92032 acts as a potent and specific T-channel antagonist in the thalamus resulting in clear cellular and circuit level effects.

METHODS

Thalamic slice preparation

Adult Sprague-Dawley rats, of either sex, were anesthetized with 50 mg/kg of pentobarbital and decapitated. Brains were blocked, removed, and immediately transferred to ice cold, oxygen equilibrated (95% O_2-5% CO_2), sucrose-cutting solution (in mM): 234 sucrose, 11 glucose, 24 $NaHCO_3$, 2.5 KCl, 1.25 NaH_2PO_4, 10 $MgSO_4$, and 0.5 $CaCl_2$. After being submerged for 2 min, brains were glued to a petri dish and sectioned into horizontal slices on a Vibratome (TPI, St. Louis, MO). Slices were bisected and trimmed to only thalamus and parts of adjacent striatum before being placed into an incubator containing artificial cerebral spinal fluid (ACSF, in mM): 124 NaCl, 5 KCl, 1.25 NaH_2PO_4, 2 $CaCl_2$, 2 $MgSO_4$, 10 glucose, and 26 $NaHCO_3$, continuously bubbled with 95% O_2-5% CO_2 at 35°C $\geq$1 h prior to recording.

Pharmacology

Na^+-dependent action potentials were blocked in some experiments by bath application of 1μM TTX (Sigma-RBI, St. Louis, MO) or inclusion of 5 mM QX-314 (Sigma-RBI) in the internal pipette solution. α-Methyl-α-phenylsuccinimide (MPS, Sigma-RBI) was dissolved in ACSF at a final concentration of 2 mM. U-92032 (provided kindly by Upjohn Pharmaceuticals, Kalamazoo, MI) was dissolved in dimethyl sulfoxide (DMSO) at a 1:1,000 stock concentration and used at a final concentration of either 1 or 10 μM.

Electrophysiology

Intracellular recordings were performed on 200-μm-thick slices gently weighed down under a nylon net and superfused with a constant flow of ACSF (2 ml/min) equilibrated with 95% O_2-5% CO_2 at 34 $\pm$ 1°C. Glass electrodes (KG-33 borosilicate glass; ID, 1.0 mm; OD, 1.5 mm; Garner Glass, Claremont, CA) were pulled in multiple stages using either a Flaming-Brown (model P-87, Sutter Instruments, Novato, CA) or a Narishige micropipette puller (model PP-830, Narishige International USA, East Meadow, NY). All recordings were made from identified neurons within the boundaries of the either the ventral posterior medial or the ventral posterior lateral thalamic nucleus (components of VB). Neurons in slices were visualized with a fixed-stage upright microscope (Axioskop, Carl Zeiss MicroImaging, Thornwood, NY) equipped with an insulated 63$\times$ objective, Nomarski optics, and an infrared-sensitive video camera (Cohu, San Diego, CA). Current-clamp recordings were obtained with an Axoclamp 2B microelectrode amplifier (Axon Instruments) using a K-gluconate filling solution (in mM): 120 K-gluconate, 11 KCl, 1 $MgCl_2$, 1 $CaCl_2$, 10 HEPES, 11 EGTA (Sigma-RBI, pH =7.3).

Voltage-clamp recordings were obtained with a List-Medical EPC-7 (patch-clamp amplifier, Darmstadt, Germany) using a cesium chloride filling solution (in mM): 135 CsCl, 5 lidocaine *N*-ethyl bromide (QX-314, Sigma-RBI), 2 $MgCl_2$, and 10 EGTA (pH = 7.3) at a holding potential of -60 mV. To improve the fidelity of the voltage clamp, we used younger animals (postnatal day 8) in which the dendrites of relay neurons are significantly less extensive than in adults (Warren and Jones 1997). All signals were filtered at 1 kHz and digitized with pClamp v.5.5 (Axon Instruments).

Thalamic oscillations

Extracellular multiunit recordings were performed on 400-μM-thick slices perfused with normal ACSF containing low Mg^{2+} (0.2 mM) and the $GABA_A$ antagonist bicuculline methiodide (BMI, 2–20 μM, Sigma-RBI) in an interface-type recording chamber. Oscillatory responses were evoked with an extracellular stimulus (20–60 V, 30 μs, 0.05 Hz) applied to the internal capsule (IC) via a bipolar tungsten electrode. Recordings were made using monopolar tungsten electrodes (1–5 MΩ) placed in RTN and VB. Signals were band-pass filtered (30 Hz–3 kHz) and digitized at 10 kHz, using Axotape, v.2 (Axon Instruments). Vehicle (0.1% DMSO) was included in all solutions (control and U-92032).

Data analysis

Single action potentials and spike trains were initiated near spike threshold (≈ -50 mV) set by DC current. A liquid junction potential of 10 mV was subtracted from all recorded membrane potentials in this study. Maximum rates of depolarization and spike train frequencies were obtained with the customized software Metatape v.14 and Spike v.5 (J. R. Huguenard), respectively. Autocorrelograms were calculated for spikes detected in extracellular multiunit recordings with time shifts over a total time window of 2–4 s with a 10-ms bin size. A modified Gabor function was fitted to the autocorrelograms by means of a simplex algorithm (Ulrich and Huguenard 1995). Data were further analyzed with Origin v.6.1 (OriginLab, Northampton, MA), and statistical significance was measured using a Student's *t*-test (Microsoft Excel 97, Microsoft, Redwood, WA). All quantitative data below are expressed as mean $\pm$ SE.

RESULTS

Low threshold spikes in ventral basal complex neurons

At physiological temperatures (33–36°C), mean resting membrane potential (-69.0 ± 0.7 mV) and mean input resistance (162.5 $\pm$ 8.8 MΩ) of VB cells ($n = 50$) were similar to values reported in previous rodent studies (Ulrich and Huguenard 1996). To assess the steady-state inactivation of T-type Ca^{2+} channels in current-clamp mode, we elicited Ca^{2+}-dependent rebound (or LTS) bursts by injecting hyperpolarizing current *prepulses* followed by a depolarizing current *push-pulse* (Fig. 1*A*) (similar to Zhan et al. 2000). We used a family

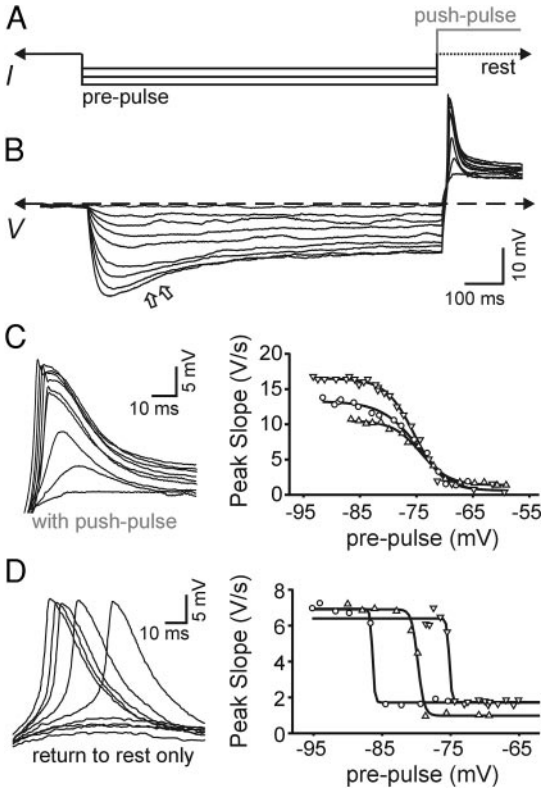

FIG. 1. Steady-state inactivation of T-type Ca^{2+} channels in current clamp mode. *A*: schematic of the current-clamp protocol used to produce a family of decrementing Ca^{2+}-dependent rebound (LTS) bursts in a ventral basal complex (VB) cell (*B*). The use of a 200-ms depolarizing push-pulse (gray solid line), instead of simply returning to rest (black dashed line), at the end of a 1-s hyperpolarizing current led to graded isolated LTSs (after TTX) whose maximum rate of rise could be used as an assay of T-channel availability (steady-state inactivation). *C*: isolated LTSs from *B* enlarged (*left*) and steady-state inactivation curves (*right*, maximum rate of LTS depolarization vs. prepulse). Three separate VB neurons, denoted by △, ▽, and ○, are shown. *D*: in the absence of the push-pulse, all or none curves, with largely variable mid-points, result in the same 3 cells (△, ▽, and ○). Arrows refer to the hyperpolarization-activated sag produced by I_H commonly seen in VB cells.

of decreasing prepulse currents beginning with a hyperpolarization to a membrane potential sufficient to de-inactivate the maximum amount of T-channels (≈ −100 mV) (Huguenard and Prince 1992). After this precondition hyperpolarization, we used a 50- to 250-pA depolarizing current push-pulse that proved to be a reliable means to activate LTS bursts. In the presence of 1 μM TTX, the addition of the push-pulse produced a robust gradation of isolated LTSs (LTS bursts in the absence of action potentials, Fig. 1, *B* and *C*), which was not possible with prepulses alone (Fig. 1*D*).

Steady-state inactivation curves were generated by plotting the maximum rate of depolarization (*dV*/*dt*; V/s) during an isolated LTS against prepulse membrane potential (mV). Prepulses were 1 s long to allow for the hyperpolarization-activated inward current (I_H) dependent sag to stabilize (McCormick and Huguenard 1992) (Fig. 1*B*, arrows). With the push-pulse protocol, plots of maximum *dV*/*dt* versus conditioning prepulse voltage produced steady-state inactivation curves that were consistent across different VB cells, and resembled those from voltage-clamp recordings in acutely dissociated VB cells (Huguenard and Prince 1992) with a mean $V_{1/2}$ of −77.2 ± 1.0 mV (n = 25; Fig. 1*C*). A protocol without a push-pulse produced sudden, all or none changes in the LTS that were not likely related to T-channel availability. Therefore all measures of the effectiveness of T-type Ca^{2+} channel antagonists in current-clamp mode were made with steady-state inactivation curves using a push-pulse protocol.

Low threshold spikes with MPS and U-92032

MPS and U-92032 both reduced the maximum LTS depolarization rate (Fig. 2, *A* and *C*). The mean maximum LTS depolarization rate in VB cells (Fig. 3, 12.2 ± 0.4 V/s, n = 25) was significantly diminished by 2 mM MPS (Fig. 3, 7.9 ± 0.7 V/s, n = 9, $P < 0.0001$) and 1 μM U-92302 (Fig. 3, 6.0 ± 0.4 V/s, n = 4, $P < 0.0001$). U-92032 (10 μM) virtually blocked the LTS altogether (Fig. 3, maximum LTS *dV*/*dt*: 1.2 ± 0.6 V/s, $P < 0.0001$, n = 7). The percent change in maximum *dV*/*dt* from control in 2 mM MPS and 1 μM U-92302 was comparable with changes in peak current amplitudes in voltage-clamp recordings made in younger animals (2 mM MPS, Fig. 2*B*: −35% vs. −52%, 1 μM U-92302, Fig. 2*D*: −51% vs. −67%) and previous studies on I_T antagonists (Avery and Johnston 1997; Coulter et al. 1990).

In addition to a clear difference in potency, MPS and U-92302 blockades exhibited several other differences described below. First, the effects of 2 mM MPS on the steady-state inactivation curve were readily reversible in all cases (Fig. 2*A*, n = 9). By contrast, a partial reversal of U-92032 effects was only seen in one cell, and that required almost 3 h of wash out. Second, the effects of 2 mM MPS were immediate, usually reaching a peak within 10–15 min, compared with the gradual, almost 1 h long, decrement observed in maximum LTS depolarization rates with 1 μM U-92032 (Fig. 2, *C* and *D*). Third, current-clamp recordings in 2 mM MPS revealed a strong reduction in LTS half-width, with almost no change in amplitude (Fig. 2*A*, *inset*). Conversely, 1 μM U-92032 applications dramatically attenuated LTS amplitude (Fig. 2*C*, *inset*). Fourth, 2 mM MPS caused a large shift in holding current in voltage-clamp recordings, while 1 μM U-92032 did not (Fig. 2, *B* and *D*).

The above differences between MPS and U-92032 suggest that MPS may be less specific and have a wider variety of effects on multiple ion channels. We next investigated the possible effects of these compounds on action potential generation in VB cells. Some drugs that block T-channels, including U-92032 and zonisamide, have also been shown to inhibit Na^+ currents (Avery and Johnston 1997; Suzuki et al. 1992). To quantify effects of U-92032 and MPS on I_{Na} in VB neurons, we used two measures: maximum rate of depolarization for near-threshold action potentials and the firing frequency versus current injection (*F*/*I*) relationship. We also examined effects on Na^+ spikes in LTS bursts using the steady-state inactivation protocol with pre- and push-pulses. In the absence of TTX, this protocol produced maximal LTS bursts with a mean of 5.1 ± 0.4 spikes (n = 30). As with recordings in TTX (Fig. 2), MPS and U-92032 had distinct effects on the shape of the LTS, primarily affecting duration (Fig. 4*A3*) and amplitude (Fig. 4*B3*), respectively. While both 2 mM MPS (n = 3) and 1 μM U-92032 (n = 2) reduced the number of spikes per LTS burst

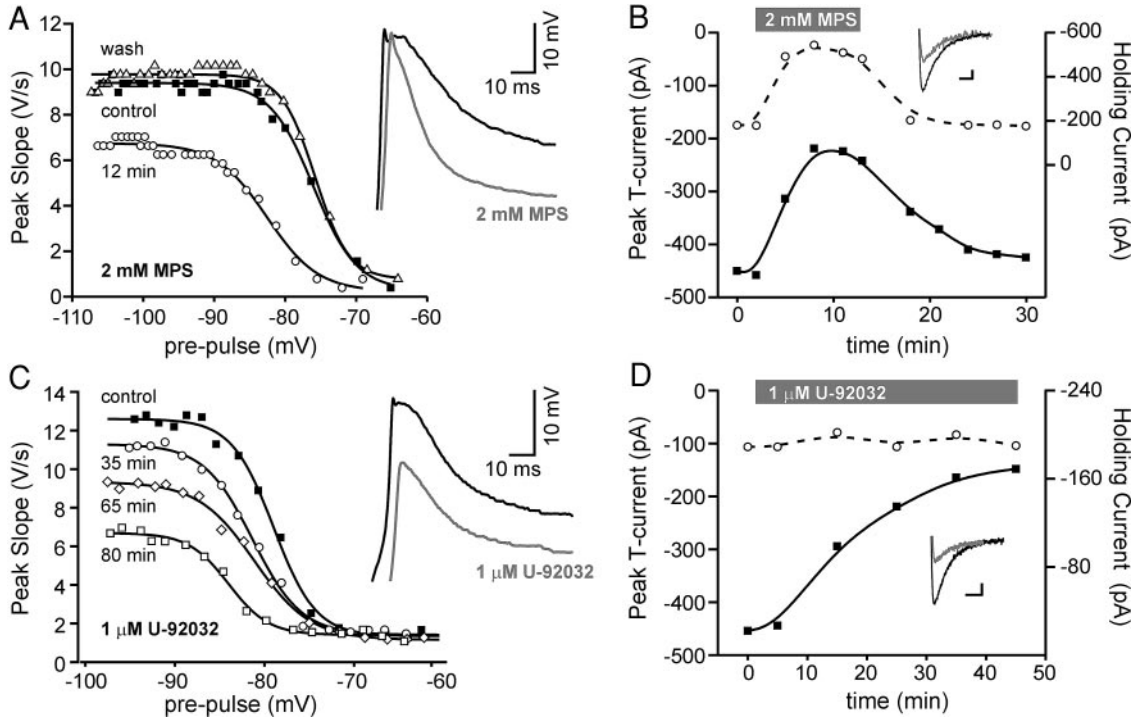

FIG. 2. Methylphenylsuccinimide (MPS) and U-92032 both inhibit T-current in VB cells. Either (*A*) 2 mM MPS or (*C*) 1 μM U-92032 significantly decreased the maximum rate of depolarization of the LTS in TTX. *A*: inhibition due to 2 mM MPS was rapid and reversible (■, control; ○, 12 min MPS; △, wash) unlike that caused by 1 μM U-92032 (*C*) (■, control; ○, 35 min; ◇, 65 min; □, 80 min U-92032). *A* and *C*: *insets* show control (black) and drug (gray) traces. These current clamp findings were paralleled in voltage-clamp recordings for both (*B*) MPS and (*D*) U-92032. Gray bars show the time period of drug applications. *B* and *D*: *insets* show T-currents in control (black) and drug (gray). Maximum T-currents in all conditions were obtained with a 1-s preconditioning period at a holding potential of −120 mV followed by a brief depolarization to −50 mV during the testing phase shown in the *insets*. Inset scale is 80 pA and 30 ms. Inset traces were aligned by their steady-state (non inactivating) current levels obtained at the end (200 ms) of the depolarization.

to one or none, MPS appeared to have a substantial effect on action potential generation itself.

Associated with the reduction of the LTS, maximum Na^+ spike depolarization rate was also significantly reduced by MPS (2 mM) from 215.4 ± 32.3 to 61.8 ± 16.7 V/s ($P < 0.05$, Fig. 4*A1*). The suppression in action potential generation by MPS (2 mM) was immediate and reversible, similar to its effect on I_T. This contrasts with the effects of U-92032 (1 μM), which also suppressed LTS bursts, but had no significant effect on Na^+ spike shape during prolonged intracellular recordings (80 min, Fig. 4*B1*). This difference was also reflected in repetitive firing: MPS severely impaired the ability of VB cells to fire spike trains (Fig. 4*A2*), while no such effects were observed with U-92032 (Fig. 4*B2*). Even at higher concentrations known to strongly inhibit Na^+ currents in hippocampal neurons (10 μM) (Avery and Johnston 1997), U-92032 appeared to have little effect on either the membrane potential (mean percentage change: −1.2 ± 2.5%, $n = 5$, $P > 0.05$), input resistance (mean percentage change: −2.4 ± 3.0%, $n = 5$, $P > 0.05$), or Na^+-dependent action potential generation (Fig. 5*A left*). Exposure to 10 μM U-92032 did not significantly affect the maximum depolarization rates of action potentials ($P > 0.05$, $n = 3$) or *F*/*I* slope (Fig. 5*B*) at times when LTS burst suppression was complete (Fig. 5*A*, *right*). There was no significant effect of 1 or 10 μM U-92032 on *F*/*I* slope after maximum inhibition in the LTS had been reached (Fig. 5*C*; control: 0.32 ± 0.03 Hz/pA vs. U-92032: 0.30 ± 0.02 Hz/pA, $n = 5$, $P > 0.05$). Maximum inhibition of the LTS was routinely achieved faster in 10 μM U-92032 (≈30 min), compared with the longer applications times necessary for 1 μM U-92032. Because the wash-in time of U-92032 is very slow, we used slice preincubations with 1 μM and 10 μM U-92032

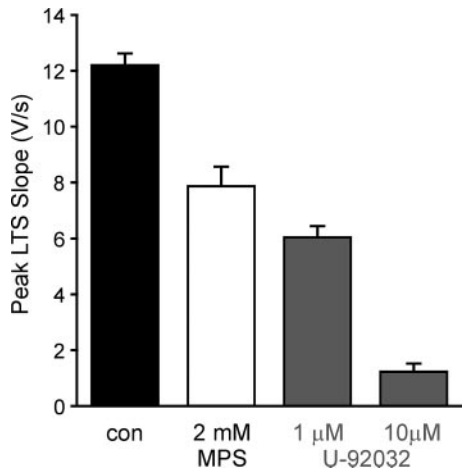

FIG. 3. Comparison of MPS and U-92032 effectiveness in suppressing T-current activity in VB cells. U-92032 (gray bars) had a greater potency than MPS (white bar) in reducing the maximum rate of depolarization of the isolated LTS. All 3 responses were significantly different from control values (black, $P < 0.0001$). All error bars show ±SE.

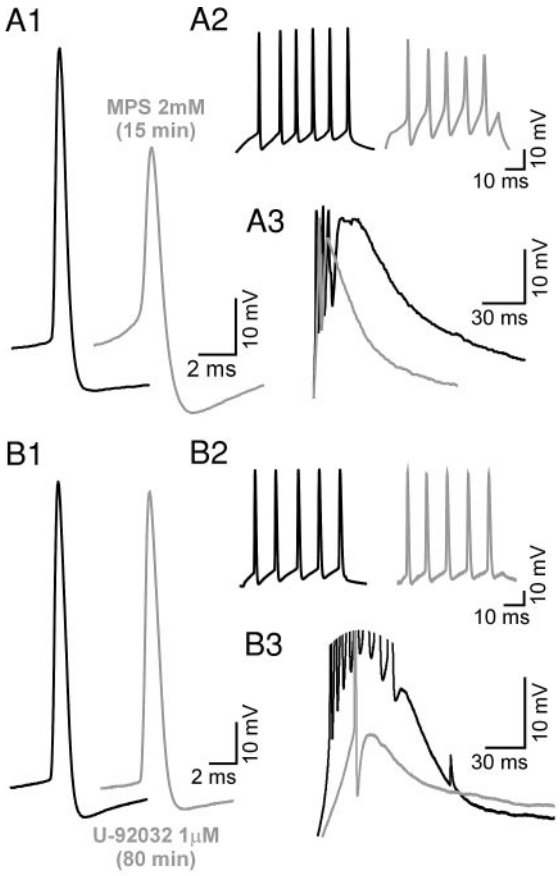

FIG. 4. MPS and U-92032 differentially affect action potential generation in VB cells. *A1*: control spike waveform and (*A2*) repetitive firing were significantly modulated by a concentration of MPS effective at suppressing LTS bursts (*A3*) in the same VB cell. Nearly double the amount of injected current used to obtain the control spike train in *A2* (*left*) was used to generate the example shown for MPS (*A2*, *right*). Unlike 2 mM MPS, 1 μM U-20332 in another VB cell significantly suppressed LTS bursts (*B3*) without severely effecting (*B1*) action potential generation or (*B2*) repetitive firing. The 2 spike trains in *B2* were obtained with identical amounts of injected current. *A* and *B*: control traces are black and drug traces are gray. Gray traces in *A* were all recorded 15 min after MPS, while those in *B* are after 80 min of U-20332.

in the following experiments to ensure equilibrium actions of drug effects.

Preincubations with U-92032

We recorded from four VB cells from slices preincubated with U-92032 from 2 to 5 h and compared their maximum action potential depolarization rates and *F*/*I* slopes to mean control values (Fig. 6). In 1 μM U-92032, two VB cells showed little qualitative changes in action potentials corresponding to a representative control, obtained after 3 h of exposure to normal ACSF (Fig. 6*A*). The maximum depolarization rate for Na^+ spikes for these two cells were 219.7 and 190.4 V/s for 2 and 3 h of 1 μM U-92032 respectively, compared with a mean control value of 200.3 $\pm$ 8.3 V/s (n = 20). *F*/*I* slopes also showed little deviation from control values (0.28 $\pm$ 0.2 Hz/pA, n = 18), with slopes of 0.23 and 0.27 Hz/pA in 2 and 3 h of 1 μM U-92032, respectively (Fig. 6*B*). With no evidence for I_{Na} modulation by 1 μM U-92032, we increased the concentration to 10 μM.

After a 2.5-h incubation of 10 μM U-92032, one VB cell demonstrated a maximum action potential depolarization rate (183.9 V/s) and *F*/*I* slope (0.26 Hz/pA), similar to mean control values. Only after 5 h of 10 μM U-92032 did we observe a VB cell with substantially impaired action potentials. Both maximum action potential depolarization rate (115.2 V/s) and *F*/*I* slope (0.13 Hz/pA) were almost one-half of mean control values. The efficacy of U-92032 on I_T in preincubations was confirmed in each cell by consistent inhibition of LTS bursts (Fig. 6*C*).

U-92032 and thalamic oscillations

Given the prominence of T-type Ca^{2+} channels in the generation of intrathalamic oscillations (Huguenard and Prince 1994b), we next investigated how U-92032 might influence the rhythmic activity recorded in acute thalamic slices. Phasic oscillations ($\approx$3 Hz) can be observed in VB and RTN multiunit recordings after an extracellular stimulation of cortical thalamic fibers running though internal capsule (Fig. 7, *A* and *B*). Application of 1 μM U-92032 progressively decreased the number of oscillatory cycles and total spike number (Fig. 7, *A* and *B*). Additionally, the period of the oscillation was modestly, but significantly, increased by 1 μM U-92032 (Fig. 7*C*). To quantify the effects of U-92032 on the thalamic oscillations, we fitted autocorrelograms to multiunit recording spike outputs with a modified Gabor function (Fig. 8*A*) (Konig 1994). The peak amplitude of the Gabor function (Fig. 8*B*), a measure of total cell firing, showed a significant reduction with 1 μM U-92032 at 15 (76.9 $\pm$ 5.4% of control, n = 22, $P < 0.001$), 30 (65.0 $\pm$ 7.7% of control, n = 22, $P < 0.001$), and 60 min (43.8 $\pm$ 7.7% of control n = 17, $P < 0.0001$). Reflecting the dose dependence seen in intracellular recordings above, 10 μM U-92032 had a larger and faster effect on amplitude demonstrated at 15 (38.7 $\pm$ 11.4% of control, n = 4, $P < 0.05$) and 30 min (10.3 $\pm$ 7.0% of control n = 3, $P < 0.005$). This dose dependence was also observed in the decay time constant (τ_D) and period of the Gabor function, representing duration and frequency of the oscillations, respectively (Fig. 8, *C* and *D*). By 30 min, 1 and 10 μM U-92032 had reached a τ_D of 81.1 $\pm$ 4.5% and 55.4 $\pm$ 17.0% of control values, respectively (Fig. 8*C*, n = 20, n = 2). The increase in period observed in Fig. 7*C* was shown in the small but significant increase in period (Fig. 8*D*) of the Gabor function for both 1 (30 min: 104.9 $\pm$ 1.1% of control, n = 20, $P < 0.001$) and 10 μM U-92032 (15 min: 110.4 + 1.5% of control, n = 4, $P < 0.01$).

DISCUSSION

In this study we have demonstrated that U-92032 can act as a T-channel antagonist in TC cells and suppress evoked intrathalamic oscillations believed to be dependent on I_T. U-92032 blocked LTS bursts recorded from TC cells at lower concentrations (1 and 10 μM) and greater magnitudes (50–90%) compared with a representative succinimide antiabsence drug (MPS). Unlike MPS, U-92032 did not interfere with action potential generation or repetitive firing until high concentrations and long exposure times were reached (10 μM and 3+ h). After establishing the intracellular effects of U-92032, we demonstrated that 1 and 10 μM U-92032 decreased the

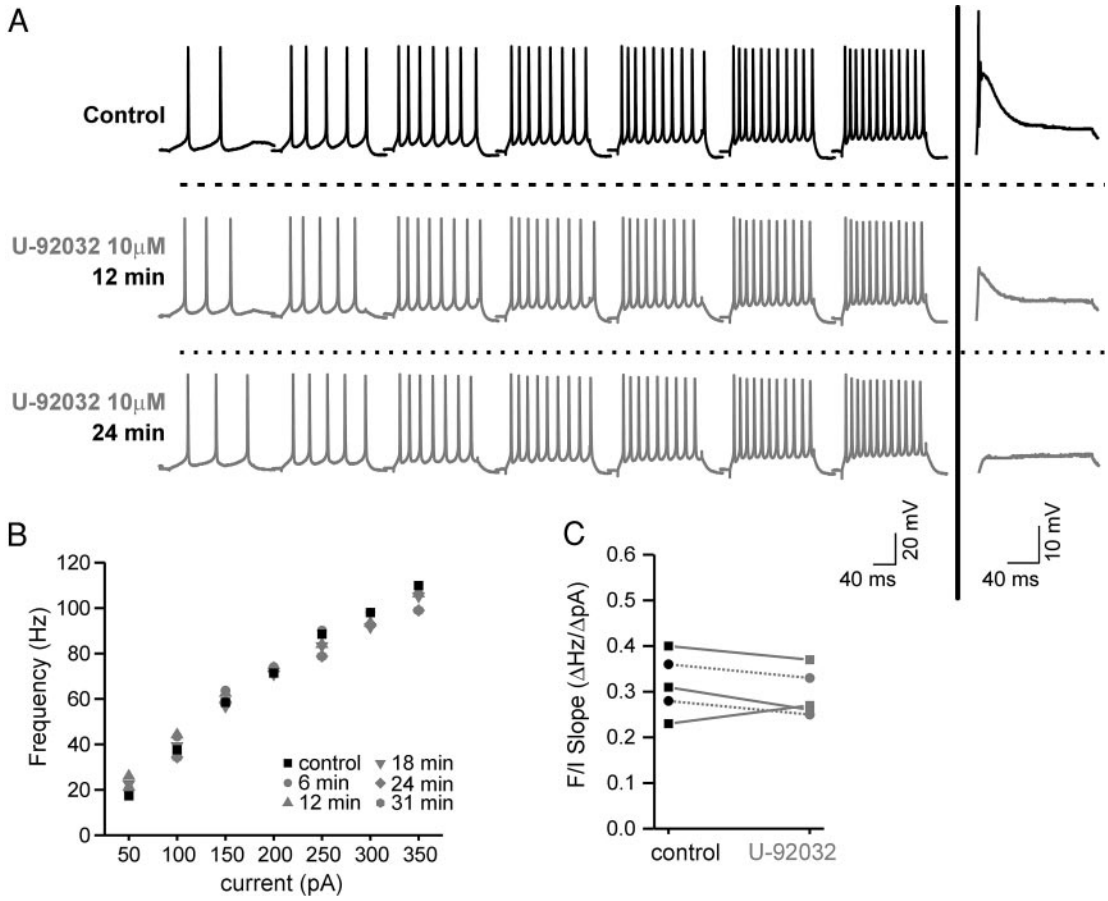

FIG. 5. U-92032 does not affect repetitive firing in VB cells. *A*: concurrent spike trains and LTS bursts from a single neuron treated with 10 μM U-92032. Horizontal rows, separated by dashed lines, contain spike trains and a LTS burst recorded at similar time points during an application of U-92032. Spike trains are aligned in columns by current injection magnitude (50–350 pA, in 50-pA increments) across all rows. *B*: frequency vs. intensity (F/I) plot for the neuron shown in *A*. *C*: summary graph showing the effects of U-92032 on F/I slope in 5 different neurons. Solid line and squares correspond to 10 μM U-92032, while dashed lines and circles correspond to 1 μM U-92032. The U-92032 point for each application was taken at a time after maximum reduction of the LTS had occurred (30 min for 10 μM, and 1 h for 1 μM U-92032). For traces and graph symbols in this figure, black and gray shading refers to control and U-92032 data, respectively.

number of cycles and overall spike count of evoked intrathalamic oscillations. These results provide further support for a central role of T-channels in epileptiform intrathalamic rhythmicity as discussed in the next section.

Advantages to current-clamp recordings

All intracellular experiments presented here were conducted in current-clamp mode, with the exception of the results shown in Fig. 2, *B* and *D*. Although this necessitated an indirect measure of I_T in the form of maximum LTS depolarization rate, we chose this paradigm for two notable reasons. First, a combination of imaging (Munsch et al. 1997; Zhou et al. 1997), physiological, and computational studies of have suggested that TC cells have a significant, if not major, contribution of dendritic T-channels (Destexhe et al. 1998). Voltage-clamp errors (Destexhe et al. 1998; Spruston et al. 1993; Velte and Miller 1996), active dendritic conductances (Williams and Stuart 2002), or simply having a significant, or distinct, population of T-channels located distally from the soma, may have contributed to the inconsistent results of ES across different preparations (e.g., acutely dissociated, cultured, in vitro slice). To be certain of the efficacy of U-92032 we based our results on an unclamped potential, recorded from TC cells believed to have a large percentage of their dendritic arborization intact.

Second, in view of a previous report showing that U-92032 inhibited voltage-dependent Na^+ channels in hippocampal CA1 pyramidal cells (Avery and Johnston 1997), we needed to confirm any possible effects on action potential generation before we could conclude the suppression of intrathalamic oscillations was primarily due to the T-channel antagonism of U-92032. In current-clamp mode, we simultaneously observed LTS bursts and tonic firing during U-92032 applications, and found essentially no effect on repetitive firing during short term ($<$2 h) applications of either 1 and 10 μM U-92032. We did not further explore the reasons for this discrepancy between results obtained in hippocampal cells (Avery and Johnston 1997) and with thalamic VB neurons in this study. It is notable that the time-dependent suppression of intrathalamic oscillations by U-92032 closely paralleled the effects on LTS inhibition, with no significant deficits in action potential generation during the same time frame.

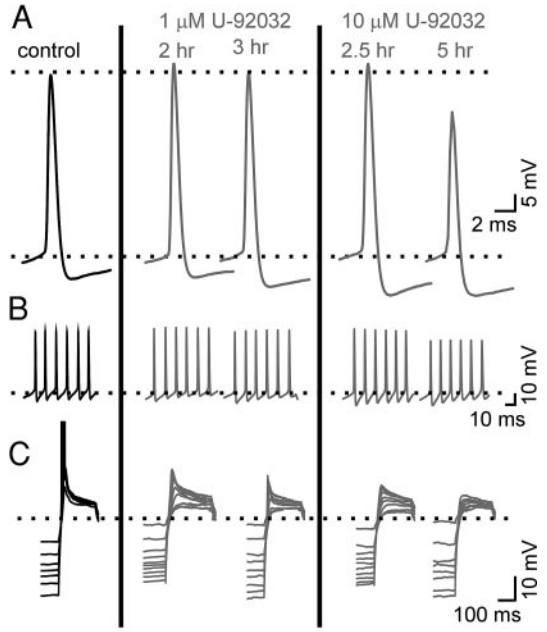

FIG. 6. Preincubation with 1 and 10 μM U-92032. Each column contains a single action potential, spike train, and family of LTS bursts all obtained from 1 representative neuron. Data from 5 cells in total are shown. At 2 or 3 h, 1 μM U-20332 (*2 middle columns*) had little effect on (*A*) action potential generation or (*B*) repetitive firing, but suppressed (*C*) LTS bursts when compared with a control cell (*left column*). Ten micromolar U-92302 at 2.5 h (*4th column*) had a similar result; however, action potential generation (*A*) and repetitive firing (*B*) were modified at 5 h (*last column*). For traces in this figure, black and gray shading refers to control and U-92032 data, respectively.

In support of a T-channel–dependent hypothesis of intrathalamic rhythmicity

Reduction in the maximum rate of LTS depolarization occurred gradually in 1 μM U-92032, usually reaching a plateau after 1 h (Fig. 2, *C* and *D*). This delay, not observed in experiments using isolated cells (Avery and Johnston 1997), was most likely caused by the lipophilic nature of U-92032 that would result in slow tissue penetration into brain slices. We also observed this slow onset in the decrease in amplitude and τ_D, and the increase in period of evoked intrathalamic oscillations after 1 μM U-92032 (Fig. 8, *B–D*). Similar dose dependence was also observed in both intracellular and extracellular recordings. U-92032 (10 μM) completely abolished both LTS bursts (Fig. 5*A*, *right*) and intrathalamic oscillations (Fig. 8*B*) quickly (<30 min), compared with the slower, and more incomplete block by 1 μM U-92032. Other cellular actions of ES have been proposed to contribute to the anti-oscillatory effects of succinimides and related compounds, including reductions in Ca^{2+}-activated K^+ and persistent Na^+ currents (Leresche et al. 1998). Such effects might alter neuronal excitability in ways independent of LTS bursts. However, we found that U-92032 had no substantial effect on single Na^+ spikes or on repetitive firing (Figs. 4 and 5), thus suggesting that the altered excitability of VB neurons produced by U-92032 resulted solely from T-current blockade. Given these results, U-92032's actions on intrathalamic rhythmicity are most likely due to inhibition of T-channels.

Although we did not specifically test for the suppression of synaptic transmission between RTN and TC cells in the presence of U-92032, the increase in period observed in intrathalamic oscillations (Figs. 7*C* and 8*D*) would argue against any decrement (Sohal and Huguenard 1998). High-threshold Ca^{2+} currents, known to support synaptic transmission, are not significantly affected by U-92032 at the concentrations used in the present study (Avery and Johnston 1997). Modeling the intrathalamic circuit shows that assuming sufficient excitatory TC→RTN synaptic activity, a decrease in the power of RTN→TC IPSCs would initially shorten the period of oscillations by reducing the time necessary for the membrane potential to repolarize to the LTS threshold (Sohal and Huguenard 1998). However, with fewer T-channels available, as would occur in the presence of U-92032, the period of oscillations should increase (cf. Figs. 7*C* and 8*D*). This follows because a reduction in T-channel availability would establishes

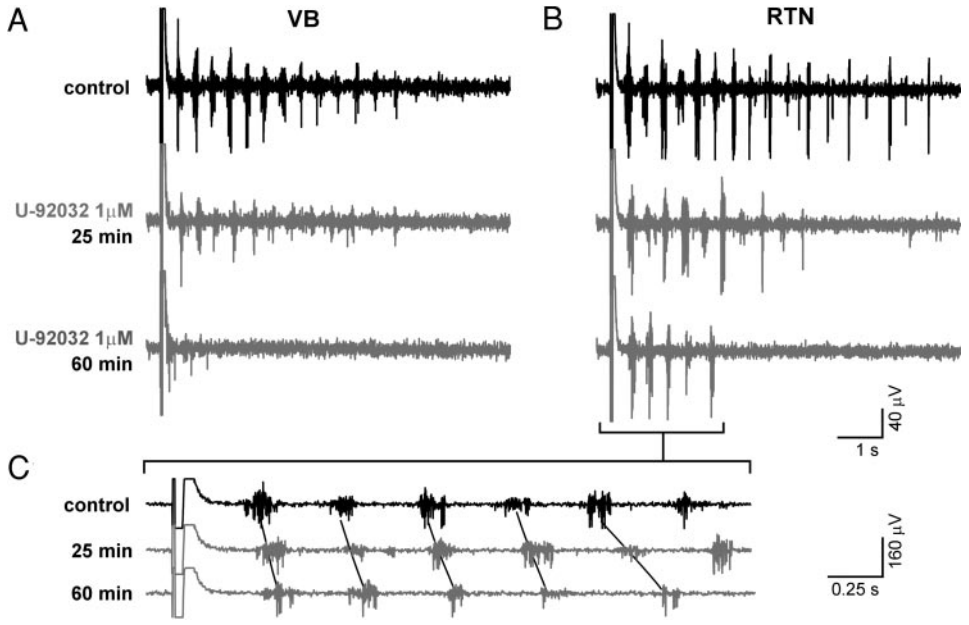

FIG. 7. U-92032 inhibits thalamic oscillations. *A* and *B*: simultaneous multiunit recordings from VB and thalamic reticular nucleus (RTN) show phasic oscillatory activity (black traces) after a brief extracellular stimulus applied to the internal capsule. 1 μM U-92032 (gray traces) progressively reduces the duration and power of this rhythmic activity, producing stronger suppression at 60 min than at 25 min. *C*: an increase in oscillation period is readily observed in expanded traces showing the first 3 s of the oscillation (brackets). Ordered burst-like activity is connected with straight lines to show a progressive slowing during long exposures to 1 μM U-92032.

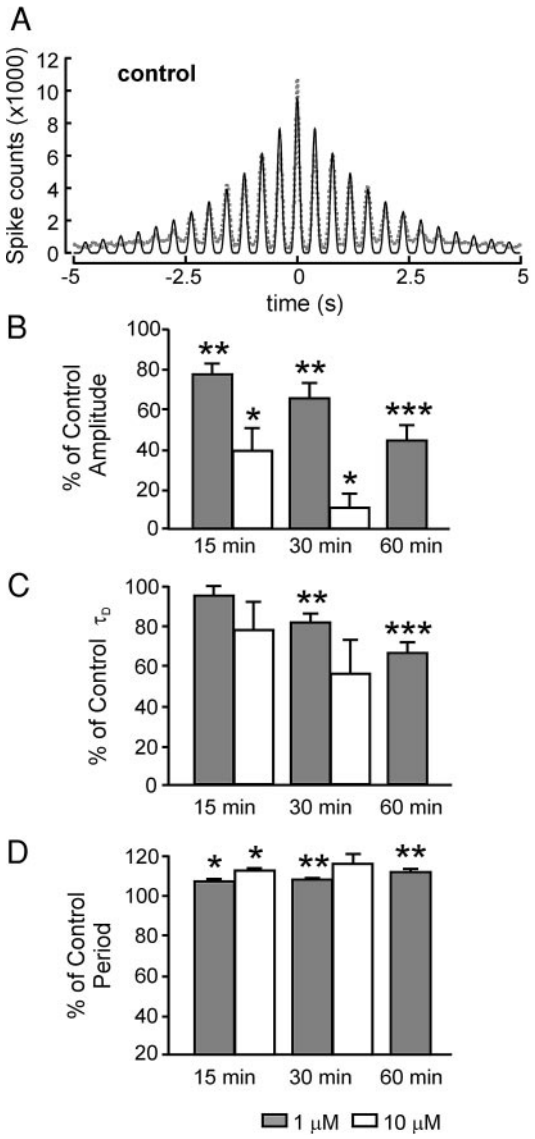

FIG. 8. Quantifying the effects of U-92032 on thalamic oscillations. *A*: autocorrelogram of multiunit spike activity in VB (gray dashed line) along with a best fitted Gabor function (black solid line). In this example, the peak amplitude, period, and decay time constant of the Gabor fit are 9,568 spikes, 395 ms, and 1,773 ms, respectively. U-92032 effects (% of control values) of (*B*) peak amplitude, (*C*) decay time constant (τ_D), (*D*) and period at 1 (gray bars) and 10 μM concentrations (white bars) are summarized in histograms. U-92032 (1 μM) has, early (15 min), late (30 min), and latest (60 min) values, while 10 μM experiments include only early and late values. All error bars show SE. *$P < 0.05$, **$P < 0.001$, ***$P < 0.0001$.

a new, more depolarized LTS threshold that would require a longer time to achieve on the termination of RTN→TC inhibitory postsynaptic potentials (IPSPs) (Bal et al. 1995; Sohal and Huguenard 1998).

Targeted antiabsence drugs

While the pharmacological control of absence seizures is effective in the majority of patients, there is still room for improvement in antiabsence therapies, with only 19% of patients completely seizure-free following treatment with one of the most commonly used antiabsence drugs, ES (Browne et al. 1975). The two most promising routes of control are *1*) augmentation of intra-RTN anti-oscillatory connections (Huguenard and Prince 1994a; Huntsman et al. 1999; Porcello et al. 2001) and *2*) block of thalamic T-type Ca^{2+} channels. Two older classes of drugs used to treat absence epilepsy, benzodiazepines and succinimides, apparently work through these mechanisms; however, improved drugs with greater efficacy and target specificity should be possible. With the recent cloning of three T-channel genes (α1G, H, and I) and the finding that a1G is the primary T-channel gene expressed in thalamus (Talley et al. 1999), it may be possible to produce a subunit-specific, and therefore location-specific, block of I_T in those suffering from absence epilepsy. We believe the present findings of a clear, and complete, block of T-channels by U-92032 associated with a strong disruption of absence-like rhythmicity will justify further efforts to exploit a T-channel–dependent hypothesis of absence epilepsy in the pursuit of new therapies.

REFERENCES

Avanzini G, de Curtis M, Panzica F, and Spreafico R. Intrinsic properties of nucleus reticularis thalami neurones of the rat studied in vitro. *J Physiol (Lond)* 416: 111–122, 1989.

Avanzini G, Vergnes M, Spreafico R, and Marescaux C. Calcium-dependent regulation of genetically determined spike and waves by the reticular thalamic nucleus of rats. *Epilepsia* 34: 1–7, 1993.

Avery RB and Johnston D. Ca^{2+} channel antagonist U-92032 inhibits both T-type Ca^{2+} channels and Na^{+} channels in hippocampal CA1 pyramidal neurons. *J Neurophysiol* 77: 1023–1028, 1997.

Bal T, von Krosigk M, and McCormick DA. Synaptic and membrane mechanisms underlying synchronized oscillations in the ferret lateral geniculate nucleus in vitro. *J Physiol (Lond)* 483:641–663, 1995.

Browne TR, Dreifuss FE, Dyken PR, Goode DJ, Penry JK, Porter RJ, White BG, and White PT. Ethosuximide in the treatment of absence (petit mal) seizures. *Neurology* 25: 515–524, 1975.

Coulter DA, Huguenard JR, and Prince DA. Specific petit mal anticonvulsants reduce calcium currents in thalamic neurons. *Neurosci Lett* 98: 74–78, 1989.

Coulter DA, Huguenard JR, and Prince DA. Differential effects of petit mal anticonvulsants and convulsants on thalamic neurones: calcium current reduction. *Br J Pharmacol* 100: 800–806, 1990.

Crunelli V and Leresche N. Block of T-type Ca^{2+} channels by ethosuximide is not the whole story. *Epilepsy Currents* 2: 53–56, 2002.

Destexhe A, Contreras D, and Steriade M. Cortically-induced coherence of a thalamic-generated oscillation. *Neuroscience* 92: 427–443, 1999.

Destexhe A, Neubig M, Ulrich D, and Huguenard J. Dendritic low-threshold calcium currents in thalamic relay cells. *J Neurosci* 18: 3574–3588, 1998.

Destexhe A and Sejnowski TJ. Synchronized oscillations in thalamic networks: insights from modeling studies. In: *Thalamus*, edited by Steriade M, Jones EG, and McCormick DA. Amsterdam: Elsevier, 1997, p. 331–371.

Gloor P and Fariello RG. Generalized epilepsy: some of its cellular mechanisms differ from those of focal epilepsy. *Trends Neurosci* 11: 63–68, 1988.

Huguenard JR. Block of T-type Ca^{2+} channels is an important action of succinimide antiabsence drugs. *Epilepsy Currents* 2: 49–52, 2002.

Huguenard JR and Prince DA. A novel T-type current underlies prolonged Ca^{2+}-dependent burst firing in GABAergic neurons of rat thalamic reticular nucleus. *J Neurosci* 12: 3804–3817, 1992.

Huguenard JR and Prince DA. Clonazepam suppresses $GABA_B$-mediated inhibition in thalamic relay neurons through effects in nucleus reticularis. *J Neurophysiol* 71: 2576–2581, 1994a.

Huguenard JR and Prince DA. Intrathalamic rhythmicity studied in vitro: nominal T-current modulation causes robust antioscillatory effects. *J Neurosci* 14: 5485–5502, 1994b.

Huntsman MM, Porcello DM, Homanics GE, DeLorey TM, and Huguenard JR. Reciprocal inhibitory connections and network synchrony in the mammalian thalamus. *Science* 283: 541–543, 1999.

Ito C, Im WB, Takagi H, Takahashi M, Tsuzuki K, Liou SY,and Kunihara M. U-92032, a T-type Ca^{2+} channel blocker and antioxidant, reduces neuronal ischemic injuries. *Eur J Pharmacol* 257: 203–210, 1994.

Jahnsen H and Llinas R. Electrophysiological properties of guinea-pig thalamic neurones: an in vitro study. *J Physiol (Lond)* 349: 205–226, 1984.

Jones EG. *The Thalamus.* New York: Plenum, 1985.

Kao CQ and Coulter DA. Physiology and pharmacology of corticothalamic stimulation-evoked responses in rat somatosensory thalamic neurons in vitro. *J Neurophysiol* 77: 2661–2676, 1997.

Kim D, Song I, Keum S, Lee T, Jeong MJ, Kim SS, McEnery MW, and Shin HS. Lack of the burst firing of thalamocortical relay neurons and resistance to absence seizures in mice lacking α1G T-type Ca^{2+} channels. *Neuron* 31: 35–45, 2001.

Konig P. A method for the quantification of synchrony and oscillatory properties of neuronal activity. *J Neurosci Methods* 54: 31–37, 1994.

Leresche N, Parri HR, Erdemli G, Guyon A, Turner JP, Williams SR, Asprodini E, and Crunelli V. On the action of the anti-absence drug ethosuximide in the rat and cat thalamus. *J Neurosci* 18: 4842–4853, 1998.

McCormick DA and Bal T. Sleep and arousal: thalamocortical mechanisms. *Annu Rev Neurosci* 20: 185–215, 1997.

McCormick DA and Huguenard JR. A model of the electrophysiological properties of thalamocortical relay neurons. *J Neurophysiol* 68: 1384–1400, 1992.

Morison RS and Basset DL. Electrical activity of the thalamus and basal ganglia in decorticate cats. *J Neurophysiol* 8: 309–314, 1945.

Munsch T, Budde T, and Pape HC. Voltage-activated intracellular calcium transients in thalamic relay cells and interneurons. *Neuroreport* 8: 2411–2418, 1997.

Porcello DM, Huntsman MM, Rudolph U, Keist R, and Huguenard JR. $GABA_A$ receptor mutant mice reveal subtype-selective benzodiazepine modulation of intra-inhibitory connections in reticular thalamus. *Soc Neurosci Abstr* 27: 491.3, 2001.

Sohal VS and Huguenard JR. Long-range connections synchronize rather than spread intrathalamic oscillations: computational modeling and in vitro electrophysiology. *J Neurophysiol* 80: 1736–1751, 1998.

Song I, Kim D, Jun K, and Shin HS. Role of T-type calcium channels in the genesis of absence seizures in the mutant mice for α1a, the pore forming subunit of the P/Q-type calcium channel. *Soc Neurosci Abstr* 27: 151.21, 2001.

Spiegel EA and Wycis HT. Thalamic recordings in man with special reference to seizure discharges. *EEG Clin Neurophysiol* 2: 23–27, 1950.

Spruston N, Jaffe DB, Williams SH, and Johnston D. Voltage- and space-clamp errors associated with the measurement of electrotonically remote synaptic events. *J Neurophysiol* 70: 781–802, 1993.

Steriade M and Contreras D. Spike-wave complexes and fast components of cortically generated seizures. I. Role of neocortex and thalamus. *J Neurophysiol* 80: 1439–1455, 1998.

Steriade M and Deschenes M. The thalamus as a neuronal oscillator. *Brain Res* 320: 1–63, 1984.

Steriade M, Deschenes M, Domich L, and Mulle C. Abolition of spindle oscillations in thalamic neurons disconnected from nucleus reticularis thalami. *J Neurophysiol* 54: 1473–1497, 1985.

Steriade M, McCormick DA, and Sejnowski TJ. Thalamocortical oscillations in the sleeping and aroused brain. *Science* 262: 679–685, 1993.

Suzuki S, Kawakami K, Nishimura S, Watanabe Y, Yagi K, Seino M, and Miyamoto K. Zonisamide blocks T-type calcium channel in cultured neurons of rat cerebral cortex. *Epilepsy Res* 12: 21–27, 1992.

Talley EM, Cribbs LL, Lee JH, Daud A, Perez-Reyes E, and Bayliss DA. Differential distribution of three members of a gene family encoding low voltage-activated (T-type) calcium channels. *J Neurosci* 19: 1895–1911, 1999.

Talley EM, Solorzano G, Depaulis A, Perez-Reyes E, and Bayliss DA. Low-voltage-activated calcium channel subunit expression in a genetic model of absence epilepsy in the rat. *Brain Res Mol Brain Res* 75: 159–165, 2000.

Tsakiridou E, Bertollini L, de Curtis M, Avanzini G, and Pape HC. Selective increase in T-type calcium conductance of reticular thalamic neurons in a rat model of absence epilepsy. *J Neurosci* 15: 3110–3117, 1995.

Ulrich D and Huguenard JR. Purinergic inhibition of GABA and glutamate release in the thalamus: implications for thalamic network activity. *Neuron* 15: 909–918, 1995.

Ulrich D and Huguenard JR. Gamma-aminobutyric acid type B receptor-dependent burst-firing in thalamic neurons: a dynamic clamp study. *Proc Natl Acad Sci USA* 93: 13245–13249, 1996.

Ulrich D and Huguenard JR. $GABA_A$-receptor-mediated rebound burst firing and burst shunting in thalamus. *J Neurophysiol* 78: 1748–1751, 1997.

Velte TJ and Miller RF. Computer simulations of voltage clamping retinal ganglion cells through whole-cell electrodes in the soma. *J Neurophysiol* 75: 2129–2143, 1996.

Vergnes M, Marescaux C, and Depaulis A. Mapping of spontaneous spike and wave discharges in Wistar rats with genetic generalized non-convulsive epilepsy. *Brain Res* 523: 87–91, 1990.

Vergnes M, Marescaux C, Depaulis A, Micheletti G, and Warter JM. Spontaneous spike and wave discharges in thalamus and cortex in a rat model of genetic petit mal-like seizures. *Exp Neurol* 96: 127–136, 1987.

von Krosigk M, Bal T, and McCormick DA. Cellular mechanisms of a synchronized oscillation in the thalamus. *Science* 261: 361–364, 1993.

Warren RA and Jones EG. Maturation of neuronal form and function in a mouse thalamo-cortical circuit. *J Neurosci* 17: 277–295, 1997.

Williams D. Study of thalamic and cortical rhythms in petit mal. *Brain* 76: 50–69, 1953.

Williams SR and Stuart GJ. Dependence of EPSP efficacy on synapse location in neocortical pyramidal neurons. *Science* 295: 1907–1910, 2002.

Xu X and Lee KS. A selective blocker for rested T-type Ca^{++} channels in guinea pig atrial cells. *J Pharmacol Exp Ther* 268: 1135–1142, 1994.

Zhan XJ, Cox CL, and Sherman SM. Dendritic depolarization efficiently attenuates low-threshold calcium spikes in thalamic relay cells. *J Neurosci* 20: 3909–3914, 2000.

Zhang Y and Noebels JL. Altered calcium currents in thalamocortical relay cells of mouse absence models with mutations of α1A and β4 calcium channel subunits. *Soc Neurosci Abstr* 27: 151.16, 2001.

Zhou Q, Godwin DW, O'Malley DM, and Adams PR. Visualization of calcium influx through channels that shape the burst and tonic firing modes of thalamic relay cells. *J Neurophysiol* 77: 2816–2825, 1997.